Research Square

Preprints are preliminary reports that have not undergone peer review.
They should not be considered conclusive, used to inform clinical practice,
or referenced by the media as validated information.

Comparative Evaluation of Observed and Predicted Erosion in Hydraulic Turbines Using IEC 62364:2019 Model

Sandeep Sagar

sagarsandeep.24@kgpian.iitkgp.ac.in

Indian Institute of Technology

Manish Pandey

Indian Institute of Technology Kharagpur

Naman Arora

Assistant Manager, Flovel Energy Private Ltd

Article

Keywords: Hydro abrasive erosion, Hydraulic turbines, IEC 62364 (2019), Kaplan turbine, Francis turbine, Pelton turbine, Sediment transport

Posted Date: August 24th, 2026

DOI: https://doi.org/10.21203/rs.3.rs-10575752/v1

License: This work is licensed under a Creative Commons Attribution 4.0 International License.
Read Full License

Additional Declarations: No competing interests reported.

Comparative Evaluation of Observed and Predicted Erosion in Hydraulic Turbines Using IEC 62364:2019 Model

Sandeep Sagar[1], Manish Pandey[2], Naman Arora[3]

[1]Research Scholar, Department of Civil Engineering, Indian Institute of Technology Kharagpur,721302

West Bengal, India. Email: sagarsandeep.24@kgpian.iitkgp.ac.in

[2]Assistant Professor, Dept. of Civil Engineering, Indian Institute of Technology Kharagpur, 721302

West Bengal, India. Email: mpandey@civil.iitkgp.ac.in (Corresponding Author)

[3]Assistant Manager, Flovel Energy Private Ltd.

New Delhi, India Email: narora@ah.iitr.ac.in

Abstract

Hydro abrasive erosion in hydraulic turbines remains a significant issue that affects the durability, reliability, and efficiency of hydropower facilities, particularly those operating in rivers with high silt content. The erosion mechanisms, modelling techniques, and predicted performance of Kaplan, Francis and Pelton turbines are thoroughly evaluated in this study. The International Electrotechnical Commission 62364 (2019) model and various semi empirical formulations are evaluated in the study, and the expected outcomes are compared with field based and experimental data. For the majority of turbine components, such as blade tips, outlets, guide vanes, and runner chambers, analysis indicates that the IEC model forecasts erosion depth and spatial distribution within ±25% of the observed values. The statistical validation results support the model's ability to accurately capture erosion behavior across a wide range of hydraulic and sediment conditions. The strong correlation (CC= 0.997, $R^2 \approx$ 0.994) indicates a close fit between predicted and observed data. Validation against the IEC

62364:2019 standard further showed that 83% of observations fell within the ±25% error band, with negligible systematic bias supporting the model's overall reliability. More sustainable and effective hydropower generation in sediment rich areas is made possible by the IEC 62364 framework, which, provides a trustworthy tool for evaluating and reducing hydro abrasive wear in turbines.

Keywords: Hydro abrasive erosion; Hydraulic turbines; IEC 62364 (2019); Kaplan turbine; Francis turbine; Pelton turbine; Sediment transport.

1. Introduction

Today, the world is facing growing challenges related to climate change, environmental pollution, and the ongoing depletion of fossil fuels, including coal, oil, and natural gas[1,2]. These concerns have intensified the need for clean, reliable alternatives to conventional energy sources [3]. Against this backdrop, hydropower has emerged as an increasingly important renewable energy source, contributing substantially to global electricity generation particularly in regions characterized by steep terrain and abundant river flow[4]. In countries such as India, Nepal, and Bhutan, as well as parts of South America and the Alps, hydropower plants are frequently situated on rivers originating in young mountain ranges. These rivers carry heavy loads of suspended sediment, including silt and sand particles rich in hard minerals like quartz and feldspar. While such rivers offer considerable hydropower potential, the sediment-laden flow they carry poses serious operational challenges for hydraulic turbines most notably, hydro-abrasive erosion[5,6].

Hydro-abrasive erosion results from repeated contact between solid sediment particles and turbine surfaces[7]. As sediment-laden water flows through a turbine, particles strike, slide, and roll across metallic components, gradually wearing away material from the surface. Over time, this leads to measurable thinning of components, increased surface roughness, and distortion

of hydraulic profiles ultimately lowering turbine efficiency while increasing vibration, noise, and maintenance demands. In severe cases, this erosion can drastically shorten the operational life of turbine components, resulting in costly shutdowns and repairs [8,9]. The severity of hydro-abrasive erosion depends on a combination of interrelated factors, including flow velocity, suspended sediment concentration (SSC), particle size distribution (PSD), particle shape, and hardness. Among these, flow velocity plays a particularly critical role, since erosion intensity rises sharply with the relative velocity between sediment particles and turbine surfaces. The properties of turbine materials and surface coatings, along with local hydrodynamic conditions such as turbulence, secondary flows, and leakage jets further shape the erosion process[10,11,12].

Different types of hydraulic turbines experience erosion in varying ways due to differences in operating head, flow regime, and geometry. For example, Francis turbines, which are widely used in medium head hydropower plants, are particularly susceptible to erosion at guide vanes, runner inlets and outlets, facing plates, and labyrinth seals, where complex three dimensional flow structures and high turbulence levels prevail[13,14,15] .Likewise, Kaplan turbines, operating under low head and high discharge conditions, commonly experience erosion at blade tips, trailing edges, and runner chambers due to high circumferential velocities and gap leakage flows[16,17]. Additionally, Pelton turbines, suitable for high head schemes, are susceptible to severe erosion at nozzles, spears, and bucket splitters due to the direct impingement of high velocity, sediment laden jets[18,12].

To understand and predict erosion related damage and to relate observed field erosion to predictive estimates [19], researchers have proposed a wide range of erosion models over the past several decades[20,18]. Early models were primarily empirical and focused on simplified relationships between erosion rate, flow velocity, and sediment concentration[15,21]. While these models offered valuable early insights, their applicability was often limited when extended to

different turbine types, materials, or sediment conditions. [22]. Later studies introduced semi empirical formulations that incorporated additional parameters such as particle size, impact angle, and material hardness, leading to improved predictions but still showing significant uncertainty under site specific operating conditions[11,23].

Recognising the need for a unified and standardised erosion assessment framework, the International Electrotechnical Commission introduced the IEC 62364[24] standard for estimating hydro abrasive erosion in hydraulic turbines. This semi empirical model explicitly accounts for SSC, PSD, particle shape and hardness, turbine material properties, and flow related parameters, and is applicable to Kaplan, Francis, and Pelton turbines[24]. As a result, the IEC 62364 framework has gained increasing acceptance and has been applied in several experimental and field based investigations to estimate erosion rates in sediment laden hydropower plants[25,26,17]. While existing studies have successfully applied the IEC 62364[24] model to individual turbine types or specific hydropower sites, the results are often reported in isolation and use different validation approaches, making cross comparison difficult. Furthermore, a critical limitation of the IEC model its assumption of linear temporal erosion progression has been noted but not systematically addressed. The present study addresses these gaps by compiles and evaluates the experimental and field based erosion data reported for Kaplan, Francis, and Pelton turbines. It evaluates the predictive capability of the IEC 62364:2019 model using a unified graphical and statistical framework across different turbine components and operating conditions. By systematically comparing IEC-based erosion estimates with observed wear reported in the literature, the study provides a quantitative assessment of the model's performance. It identifies consistent trends, strengths, and limitations across different turbine classes. In contrast to existing reviews that primarily focus on erosion mechanisms or modelling concepts, the present work emphasises direct comparison

between predicted and measured erosion, thereby supporting a clearer understanding of the applicability of the IEC framework in sediment laden hydropower systems.

Therefore, the objective of this study is to systematically compile published experimental and field based erosion data for Kaplan, Francis, and Pelton turbines and to compare these observed erosion values with predictions obtained using the IEC 62364:2019 model. The predictive performance of the IEC framework is evaluated using graphical and statistical methods, and its strengths and limitations are discussed in comparison with other erosion models reported in the literature. By bringing together a consolidated, quantitative assessment, this study seeks to support better erosion prediction, inform turbine design decisions, and guide effective sediment management strategies for hydropower plants operating under sediment-laden river conditions..

2. Erosion in Hydraulic Turbines

Sediment induced erosion is widely recognised as one of the most critical degradation mechanisms affecting hydraulic turbines operating in sediment laden rivers. The problem is particularly severe in mountainous and geologically active regions, where rivers transport large quantities of hard mineral particles, such as quartz and feldspar, generated by weathering and glacial processes[27]. In reaction turbines, especially Francis turbines, high internal velocities and complex secondary flow structures intensify particle surface interactions, rendering runner blades, guide vanes, and clearance regions particularly vulnerable[28]. In contrast, impulse turbines such as Pelton machines experience concentrated hydro abrasive damage at bucket splitters and injector nozzles due to direct high velocity jet impingement[29], as demonstrated in Figure 1 presents a new and severely eroded Pelton turbine runner buckets, highlighting significant profile degradation due to prolonged hydro abrasive sediment exposure similarly Figure 2 shows distinct erosion zones and altered surface morphology are observed on the

Pelton turbine nozzle and spear under hydro abrasive operating conditions. Despite geometric differences, sediment erosion consistently emerges as a dominant performance limiting mechanism across turbine technologies.



Figure 1 Comparison of new and severely eroded Pelton turbine runner buckets showing profile degradation due to hydro-abrasive sediment wear [30]

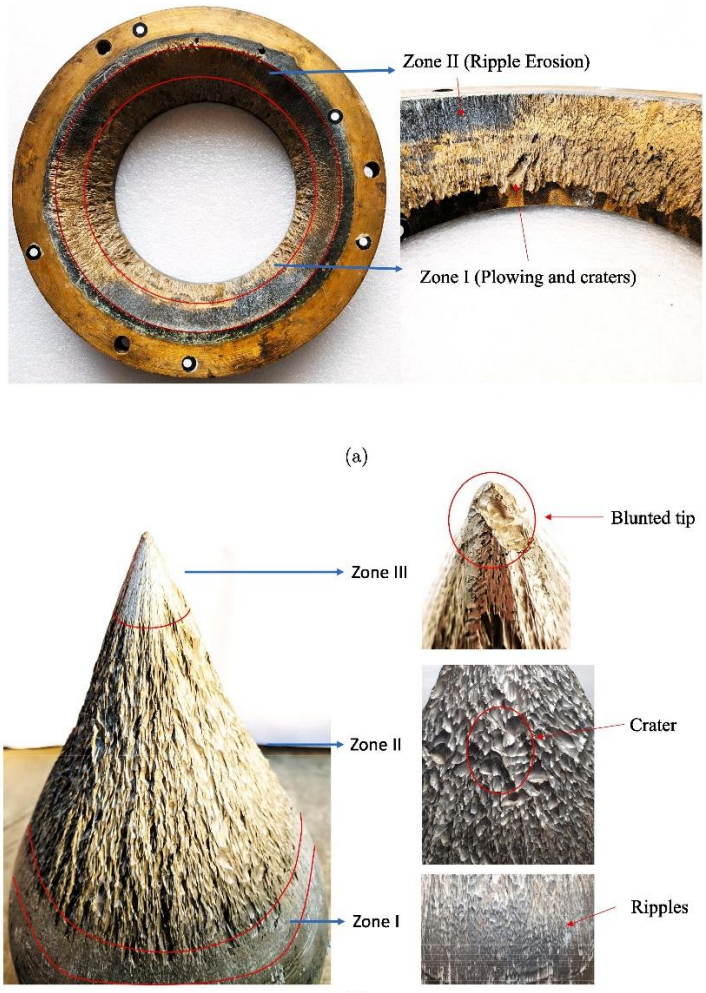


FIGURE 2 Erosion zones and surface morphology of the Pelton turbine nozzle and spear under hydro-abrasive conditions [31].

Field observations and experimental investigations confirm that erosion produces measurable material loss even over relatively short operational durations. Progressive wear alters blade curvature, enlarges clearance gaps, and intensifies leakage flows, thereby modifying internal pressure distributions and reducing hydraulic efficiency[27]. Numerical analyses further demonstrate that erosion within the guide vane clearance regions strengthens leakage vortices and secondary flows, thereby amplifying particle acceleration and impact severity[32]. Thus, sediment erosion should be considered a performance related problem rather than only a surface damage phenomenon.

From a mechanistic standpoint, sediment erosion arises from repeated particle surface impacts governed by impact velocity, impingement angle, particle size, hardness, and material mechanical properties[33]. Erosion rate increases nonlinearly with particle kinetic energy, reflecting the energy driven nature of material removal[34]. The impingement angle determines the dominant wear mechanism: shallow angles promote ductile micro cutting and ploughing, whereas near-normal impacts induce brittle fracture and surface fatigue. Microstructural analyses reveal mixed ductile brittle behaviour depending on particle angularity and impact conditions, demonstrating that erosion severity cannot be characterised solely by sediment concentration but must be interpreted through particle mechanics and material response[35] To resolve the spatial localisation of erosion within complex turbine geometries, multiphase computational fluid dynamics (CFD) modelling has become indispensable. Contemporary approaches employ Euler Lagrange particle tracking coupled with erosion models to predict particle trajectories, impact frequencies, and erosion rate contours[36] Experimental investigations on Pelton buckets further indicate that erosion severity increases proportionally with suspended sediment concentration (SSC) and median particle size (d_{50}), while coarse particles tend to produce localised craters and pits, particularly along bucket depth and splitter regions[23,18].

In Francis turbines, erosion hotspots consistently coincide with leakage vortices, secondary flow structures, runner trailing edges, and regions of the guide vane pressure sides where localised hydrodynamic disturbances amplify particle velocity and promote near normal impacts[32,36]. Additionally, Figure 3 shows sediment erosion significantly affects the runner blades, particularly at the leading and trailing edges, where repeated particle impacts result in surface degradation and alteration of the blade profiles[37].

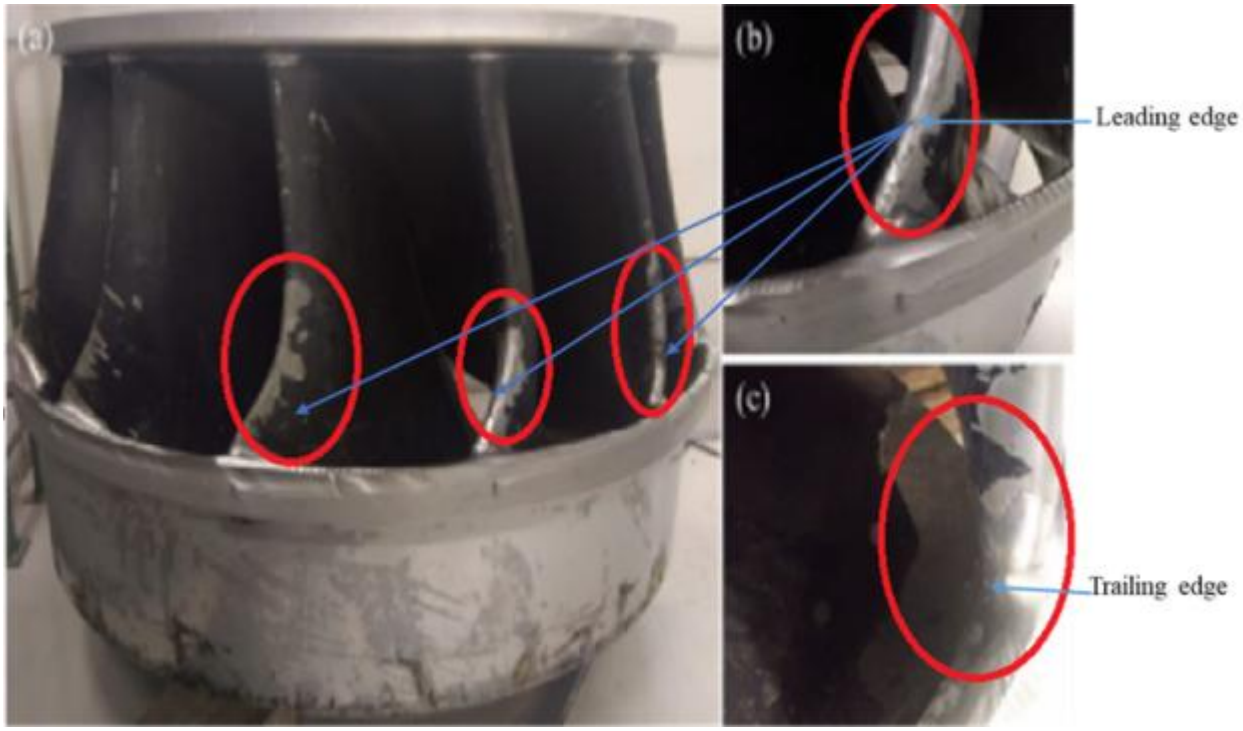


Figure 3 Sediment induced erosion on the Francis turbine runner at Middle Marsyangdi Hydropower Plant: (a) overall runner condition, (b) leading edge damage, and (c) trailing edge wear [38]

Representative localised erosion patterns on Francis turbine runner blades: (a-b) leading edge impact erosion, (c) mid chord surface wear due to sediment interaction, and (d) trailing edge damage near the lower ring caused by combined hydrodynamic and abrasive effects. Similar Lagrangian simulations in Kaplan turbines report severe erosion at the blade leading edges and in the hub region, driven by three dimensional flow effects and clearance induced disturbances[39]. Collectively, these observations suggest that localised flow behaviour plays a dominant role in governing erosion patterns, whereas bulk sediment concentration alone does not adequately explain the distribution of material loss. Figure 4 presents a field photograph of the Kaplan turbine runner at Bhudkalan Hydropower Plant, highlighting severe sediment induced erosion on the blade surface. Noticeable material loss appears along the leading and trailing edges, pointing to continuous exposure to sediment-laden flow. The erosion has

resulted in edge thinning and surface roughening, which may reduce efficiency and degrade hydraulic performance [17].



Figure 4 Erosion damage on Kaplan turbine runner blade showing material loss along the leading and trailing edges at Bhudkalan HPP [17].

The interaction between sediment erosion and cavitation further complicates the degradation process. Cavitation bubble collapse generates localised high pressure micro jets and shock waves that weaken surface integrity, thereby increasing susceptibility to subsequent abrasive impacts. The combined sediment cavitation mechanism has been shown to produce more severe material damage than either mechanism acting independently[40]. This synergistic behaviour is particularly critical in high velocity regions such as blade trailing edges and leakage paths.

Material properties play a decisive role in erosion resistance. While surface hardness contributes to improved wear resistance, other properties such as fracture toughness, elastic modulus, and microstructural stability also significantly influence erosion behaviour[35]. As a

193 result, surface engineering strategies, including advanced alloys and thermal spray coatings,
194 have been investigated as ways to mitigate hydroabrasive degradation[28]. Laboratory studies on
195 tungsten carbide cobalt chromium coatings applied using high velocity oxy-fuel (HVOF)
196 techniques have shown notable reductions in erosion rate compared with uncoated martensitic
197 stainless steels under slurry impact conditions[41]. That said, coating performance remains
198 sensitive to impact angle, particle hardness, and local hydrodynamic conditions, pointing to the
199 need for site-specific material optimisation[29].

200 Beyond localised surface wear, sediment erosion influences long term structural integrity and
201 service life. Progressive surface roughness increases hydraulic losses and alters stress
202 distributions under cyclic loading conditions. In modern renewable energy systems, where
203 hydropower plants operate under increasingly flexible and variable regimes, erosion induced
204 geometric modifications may accelerate fatigue damage and reduce operational lifespan[42].
205 Therefore, erosion must be evaluated within an integrated durability framework that combines
206 hydraulic performance, material degradation, and structural reliability considerations.

207 In engineering practice, empirical formulations serve as a complement to experimental and
208 numerical methods. The IEC 62364 [24] guideline offers a standardised approach for estimating
209 erosion depth based on particle load, relative velocity, material coefficients, and geometric
210 scaling parameters, with particular emphasis on the strongly nonlinear relationship between
211 erosion and flow velocity. Unlike earlier empirical correlations, which mainly accounted for
212 SSC and particle size distribution (PSD), the IEC 62364 [24] framework goes further by
213 incorporating particle shape, hardness ratio, and exposure duration into the particle load
214 formulation — offering a more comprehensive representation of sediment-induced wear
215 mechanisms. Such frameworks support practical risk assessment in sediment prone

hydropower environments. Equations (1a) and (1b) from IEC 62364 can be used to estimate the erosion depth S (mm) in the hydraulic turbine caused by silt and particle load.

$$S(mm) = P_l \times u^{3.4} \times K_m \times \frac{K_f}{RS^p} \quad (1a)$$

where the particle load (P_l) is expressed as:

$$p_l\left(\frac{kg}{m^3}\right) = \sum_{i=1}^{n} c_i \,.\, K_{size,i} \,.\, K_{shape,i} \,.\, K_{hardness,i} \,.\, t_i \quad (1b)$$

Here, u represents the relative velocity between the sediment-laden flow and the turbine surface, K_m accounts for material resistance, and K_f reflects local flow-related effects. The particle load term integrates sediment concentration, particle size, angularity, hardness ratio, and exposure duration. The reference size RS and exponent p describe geometric scaling effects associated with curvature. This formulation highlights the strong nonlinear dependency of erosion depth on flow velocity and sediment characteristics, reinforcing the importance of accurate sediment and velocity characterisation in erosion-prone hydropower environments (IEC 62364, 2019).

Overall, sediment erosion in hydraulic turbines is a multiscale, multiphysics degradation process governed by particle impact mechanics, complex internal hydrodynamics, evolving surface geometry, and material response [43]. Although significant advances in experimental diagnostics and high fidelity CFD modelling have enhanced predictive capability, accurate long term durability assessment requires integrated consideration of flow behaviour, sediment characteristics, material resistance, and geometric evolution under operational conditions. Continued coupling of field validation, geometry evolving simulations, and site specific material optimisation is therefore essential to ensure sustainable turbine performance in sediment-rich hydropower environments.

3. Existing equation of the Erosion model

The IEC 62364[24] (2019) standard provides a semi empirical model for evaluating hydro abrasive erosion in hydraulic turbines, which is mentioned in Equation (1a)&(1b)

To improve component level predictions[44], a velocity concentration based model was developed, expressed in its general form as given in Equation. (2a)-(2e):

$$E = f.W^n.C_s^m \quad (2a)$$

$$E = \Delta m/t\ erosion \quad (2b)$$

E is the erosion rate, W is the resultant velocity, and C_s is the sediment concentration. They further provided component specific equations for Pelton turbines.

$$E = 5.45 \times 10^{-9} \times V^{3.16} \times C^{0.98}\ (Erosion\ at\ the\ Nozzle\ tip) \quad (2c)$$

$$E = 1.47 \times 10^{-9} \times V^{3.41} \times C^{1.02}\ (Erosion\ at\ the\ needle\ shaft) \quad (2d)$$

$$E = 8.82 \times 10^{-9} \times V^{3.51} \times C^{1.01}\ (Erosion\ at\ the\ runner\ bucket) \quad (2e)$$

These formulations demonstrated that erosion is extremely sensitive to velocity (exponents ranging from 3.16 to 3.51), while concentration plays a nearly linear role. This marked a significant step beyond the IEC model by showing how different turbine parts respond differently to erosive wear.

While IEC and Liu's models emphasise velocity and concentration, Mansouri's model [45] focuses on material hardness and impact angle. It defines the erosion rate as shown in Equation (3a)-(3d).

$$ER = KF_S V_P^{2.41} F\ (\theta) \quad (3a)$$

With the angular function:

$$F(\theta) = \frac{1}{f}(\sin\theta)^{n_1}\ (1 + Hv^{n_3}(1 - \sin\theta))^{n_2} \quad (3b)$$

And the material factor:

$$K = C(BH)^{-0.59} \quad (3c)$$

$$BH = \frac{HV + 0.1023}{0.0108} \quad (3d)$$

here, V_P is particle impact velocity, F_S Sharpness factor, and BH and HV represent Brinell and Vickers hardness. By explicitly including hardness and impact angle, this model emphasises that sediment angularity and surface resistance strongly govern erosion.

A similar idea was expanded in the Oka model[46] as given in Equation (4a)-(4c), which considered erosion at arbitrary impact angles by relating it to erosion at normal incidence (90°)

$$ER = ER_{90} g(\theta) \quad (4a)$$

$$ER_{90} = K_p (Hv)^{K_1} (Vp)^{K_2} (dp)^{K_3} \quad (4b)$$

$$g(\theta) = (sin\,\theta)^{n_1} (1 + Hv(1 - sin\,\theta))^{n_2} \quad (4c)$$

This approach provided a systematic way of including hardness (H_V), velocity (V_p) and particle size (d_p), while capturing the angular dependency of erosion, which is critical in components such as guide vanes and runner blades.

Later, Zhang et al[35] the modified the angle function to improve agreement with experimental data[48]. The proposed model is mentioned in Equation (5a) & (5b)

$$ER = 2.17 \times 10^{-7} (BH)^{-0.59} F_S V_p^{2.41} F(\theta) \quad (5a)$$

with a polynomial expression for the impact angle

$$F(\theta) = 5.4\theta - 10.11\theta^2 + 10.93\theta^3 - 6.33\theta^4 + 1.42\theta^5 \quad (5b)$$

This refinement captured erosion variation more accurately across angles, while retaining the hardness factor (BH) and particle sharpness term (F_s).

The Neilson Gilchrist model [49] provided a more mechanistic view by separating erosion into cutting and deformation wear. The total erosion rate is given in Equation (6a) & (6b):

$$ER = ER_C + ER_D ER_C = \begin{cases} \dfrac{V_p^2 \cos^2\theta \sin\dfrac{n\theta}{2\theta_0}}{2ec} & , \quad \theta < \theta_0 \\ \dfrac{V_p \cos^2\theta}{2\varepsilon c}, \end{cases} \tag{6a}$$

and deformation wear expressed as:

$$ER_D = \frac{max\left(V_p \sin\theta - K_{D,}0\right)^2}{2\varepsilon_c} \tag{6b}$$

here $\theta_c = 45^\circ$ is the transition angle, while ε_c is the cutting deformation coefficient. This model uniquely recognises the dual nature of erosion, where shallow angles promote cutting steeper angles promote deformation.

4. Data Description

Turbine erosion is widely recognised as a critical challenge in hydropower plants, as it directly reduces turbine performance, efficiency, and operational lifespan[15]. However, the availability of systematic erosion related datasets remains relatively scarce, with only a limited number of researchers documenting experimental or field based evidence. For this study, relevant literature was compiled, encompassing Kaplan, Francis, and Pelton turbines, highlighting different erosion mechanisms and affected components. In the case of Kaplan turbines, which operate under low head and high flow conditions, tend to show erosion concentrated at the points where the flow interacts directly with the blades — areas where sediment-laden water gradually wears away material over time Arora et al.[17] observed this damage at the blade tip, outlet, and chamber, shedding light on how erosion develops under real operating stresses Rai & Kumar[16] reported comparable findings, noting erosion at the blade inlet, outlet, and turbine chamber, which further confirms that both the leading and trailing edges of the blades remain

particularly susceptible to damage. Francis turbines, being the most widely deployed in medium-head schemes, have received considerably more attention in the literature and show multi-component erosion patterns affecting both stationary and rotating elements. Sangal et al[26] reported erosion at the guide vane, runner inlet, runner outlet, runner chamber, and labyrinth seal, while Acharya et al[25] validated these findings and went further, identifying erosion at the facing plate as well — a reminder that erosion is not limited to the main runner passages but extends to auxiliary surfaces too. Sharma et al[50] provided additional detailed documentation of erosion in Francis turbines, consistently reporting damage at the guide vane, runner inlet, runner outlet, and labyrinth seal, which helps establish a strong comparative basis across different sites and operating regimes. Pelton turbines, by contrast, experience erosion primarily due to high-velocity, sediment-laden jets striking the buckets. Rai et al[51] presented experimental observations quantifying erosion across different operating durations a valuable contribution, since it yields time-dependent erosion rates that are critical for predicting wear progression and planning maintenance schedules. Adding to this body of work, Thapa et al[9] reported further findings for Francis turbines, identifying erosion at the guide vane, runner inlet, and runner outlet, reinforcing these locations as consistent erosion hotspots across multiple studies. Collectively, the reviewed studies emphasize that Kaplan turbines are predominantly vulnerable at blade tips, inlets, and outlets due to direct flow interactions, Francis turbines undergo widespread multi component erosion involving guide vanes, runner passages, and labyrinth seals, while Pelton turbines exhibit bucket surface degradation that intensifies with operating time and sediment load; however, despite these contributions, significant research gaps persist, particularly the scarcity of long term field data, the limited availability of quantitative erosion rate measurements, and the absence of standardized reporting protocols, all of which hinder reliable cross study comparisons.

5. Methodology for IEC 62364:2019 Model Application

The application of the IEC 62364:2019 model to the compiled dataset followed a systematic procedure. First, source studies were selected on the criterion that they either explicitly reported the key IEC 62364:2019 input parameters or provided sufficient operational and sediment data to permit their back-calculation. The primary input parameters extracted or derived for each case study were: (i) the characteristic relative velocity (u, m/s) at each turbine component, estimated following the IEC 62364:2019 velocity coefficient charts using turbine-specific design parameters (head, discharge, specific speed, runner diameter) as reported by the respective source study; (ii) the material resistance coefficient (Km), taken from values prescribed by the standard for the reported turbine material — for martensitic stainless steel 13Cr4Ni, Km = 1.0 was adopted as the reference; (iii) the flow coefficient (K_f) and the reference size exponent (p, R_s), which govern the geometric scaling of erosion depth and were assigned per the turbine-type-specific guidance in IEC 62364:2019; and (iv) the particle load (P_l in $Kg.h/m^3$), computed from sediment concentration (SSC, mg/L), median particle diameter (d_{50}), particle shape factor (K_{shape}), mineral hardness correction ($K_{hardness}$), and operational duration (t, h), as reported by each source study. Where mineral composition was available via X-ray diffraction (XRD) analysis as in Arora et[17] althe hardness correction was applied precisely; where mineralogical data were absent, a conservative Khardness corresponding to quartz-dominated sediment (Mohs hardness ≥ 7) was assumed and clearly noted. All assumptions and default values adopted in each case study are documented in Table 1, which summarises the key input parameters and observed erosion values across all six case studies included in the graphical and statistical validation.

350 **Table 1** : **Summary of IEC 62364 Input Parameters across Hydro-Abrasive Erosion Case Studies**

Study / Turbine Type	**HPP Location**	**Net Head (m)**	**SSC Range (ppm)**	**D_{50} / K_{size} (mm)**	**K_{shape}**	**$K_{hardnes}$**	**K_m**	**W (m/s)**	**K_f & p**	**P_L (kg·h/m³)**
Rai et al[56] Pelton Turbine	Toss HPP Himalayas, India (1:8 scale model)	140–200 (model)	750, 1500, 3000	0–355 µm (4 PSD classes)	Inferred from sediment analysis	Not quantified separately	K_m=1 (13Cr-4Ni) Km>1 (Bronze) Km<1 (WC-Co-Cr)	22.05–32.11 (relative bucket velocity)	Power-law empirical ($K \cdot SSC^a \cdot d_{50}^b \cdot V^c \cdot t^d$) V exp. c: 3.10–4.09	Not calc.; SSC integrated 3–12 h exposure
Arora et al[17] .Kaplan Turbine	Mohammadpur HPP Upper Ganga Canal, India (9.3 MW)	5.48	2450–5300 (max; 2007–2011)	0.174 (sieve analysis)	1.42 (semi-angular; DIA)	0.86 (XRD; quartz 69.58% feldspar 8.34%)	1.0 (13Cr-4Ni)	W_{tip}=33.73 W_{out}=37.64 W_{ch}=15.56 W_{gv}=5.04	Blade tip & outlet: GV K_f calibrated (CF: 3.55×10^{-8}–1.75×10^{-5})	356.87 (annual avg.; daily SSC 2007–2011)
Rai & Kumar[57] Pelton turbine	Toss HPP, Tosh River, Indian Himalayas 2 × 5 MW Q = 3.5 m³/s per turbine	174	750, 1500 and 3000	d_{50} avg = 27 µm (range d_{50}: 20–40) broad PSD)	~1.6 (avg) f_R = 0.40 (round) (1–f_R) = 0.60 (angular) b/l avg = 0.74 Roundness avg = 0.84	Uncoated (13Cr-4Ni, Mohs ~4.5): 0.88 (88% minerals harder	6.25×10^{-13} (13Cr-4Ni 1.38×10^{-14} 13Cr-4Ni + WC-Co-Cr HVOF	(22.05, 25.62, 28.97 and 32.11) for different condition	K_f is 1 for rounded or 2 for angular and value of P is not properly mentioned	Uncoated: 73.4 kg·h/m³ (K_{size} weighted) 40.3 kg·h/m³ (K_{size} = d_{50} only)

					CV b/l = 1.6% CV roundness = 1.3%	than steel) Coated (WC-Co-Cr, Mohs 6.5–7): 0.73 (65–77% minerals harder than coating)				Coated: 60.9 kg·h/m³ (K_{size} weighted) 33.4 kg·h/m³ ($K_{size} = d_{50}$ only) Op. hrs: 3180 h SSL: 12,540 t
Sangal et al[26].Francis Turbine	Maneri Bhali-II HPP Bhagirathi R., India (304 MW; 4×76 MW)	247.3	250–5000 (max 5810 monsoon 2018)	0.15 (LISST portable XR)	2.0 (angular; IEC default)	0.90 (quartz >95%; high abrasivity)	1.0 (13Cr-4Ni)	W_{run}=35.48 W_{gv}=25.37	Runner in: 0.90×10^{-6}; p=0.25 Runner out: 0.54×10^{-6}; p=0.75 GV: 1.06×10^{-6} Labyrinth: 0.38×10^{-6}; p=0.75	1114.76 (max; Unit 2 FY 2018–19; 5026 op. h)
Sharma et al[50]. Francis Turbine	Bhilangana-III HEP Himalayas, India (3×8 MW; horizontal)	210	Avg - 460 (monsoon) Max 2049 (29,291 t / 6993 h)	Approx. 90% <300 µm ~76% <200 µm (dry sieve; d_{50} est.)	SF=0.75 (SEM+ImageJ; Cox relation; n=40)	SiO_2 ~90 wt% (Mohs 7; EDX) High quartz → high K_h	1.0 (CA6NM) HP-HVOF WC (Km<1) SS 410 facing plates	CFD-derived relative velocities (Tabakoff erosion	K_f not computed; CFD (Tabakoff model; Teran et al. constants)	Not calc. as IEC PL; Total: 29,291 MT Avg rate: 4.19 t/h

								model; not IEC)		
Rai et al[51].Pelton Turbine (Test Rig Design)	Proposed test rig (IIT Roorkee) based on Toss HPP	~200 (V_{jet}: 60–70 m/s)	500–3000 (designed range)	0–355 µm (4 sieve classes; site samples)	1.5 (assumed; angular; IEC default)	0.73 (assumed; HPP mineral content)	1.0 (assumed; 13Cr-4Ni)	~30–35 (design jet velocity 60–70 m/s)	K_f=1.0×10⁻⁶ (assumed) RS exp. p=0.25 (assumed) [Not in IEC for Pelton at time of study]	11.17–67.01 (est. from SSC; 48 h test cycles)
Acharya et al. 2022 (Francis)	Bhilangana-III HPP, India	207	Not explicitly stated — particle load derived from site sampling data; 229 hr operating period used for comparison	Not given (only mineralogical % reported, no grain-size figure)	Not reported	Not reported (only Moh's hardness of minerals: Quartz 7, Feldspar 6–6.5, Hornblende 5.5, Magnetite 5.5–6.5)	1 (guide vanes/runner: martensitic steel CA6NM/13Cr4Ni)	W_{run} = 32.26; W_{gv} = 35.05	Guide vanes: K_f=1.06×10⁻⁶, p=0.25 Facing plates: K_f=0.86×10⁻⁶, p=0.25 Runner inlet: K_f=0.90×10⁻⁶, p=0.25 Runner outlet: K_f=0.54×10⁻⁶, p=0.75 Labyrinth seals: K_f=0.38×10⁻⁶, p=0.75	Not given as an explicit numeric value in text (stated as "calculated based upon sampling data," feeding directly into S)

Sangal et al. 2025 (Francis)	Maneri Bhali-II (MB-II) HPP, Uttarkashi, Uttarakhand, India	247.3 (gross discharge 142 m^3/s)	Site data used for FY2018–19 modeling; shutdown threshold >3000 ppm; PSI sensitivity range: 1000, 2000, 3000, 4000, 5000 ppm	Size factor exponent = 0.25 (applied to d_{50} in mm); PSI silt-size range: 90, 110, 130, 150 µm (0.09–0.15 mm)	PSI range: 0.5, 0.65, 0.8, 1.0	Not given a numeric value	1 (13Cr–4Ni martensitic steel, reference material)	PSI range: 36.0, 36.6, 37.5, 38.2 (best alternative P-2: 36.6)	Guide vanes: $K_f=0.9\times10^{-6}$, p=0.25 Runner inlet: $K_f=0.54\times10^{-6}$, p=0.25 Runner outlet: $K_f=1.06\times10^{-6}$, p=0.75 Labyrinth seals: $K_f=0.38\times10^{-6}$, p=0.75	Not given as an explicit numeric value (used internally to compute cumulative erosion in Table 2, but PL itself not tabulated)

The accuracy of the IEC 62364:2019 predictions was evaluated using two complementary approaches: (i) graphical comparison, in which IEC-computed erosion depth was plotted against observed erosion depth on a 1:1 axis with ±25% error envelopes (Figure 5, panels a–f), one panel per source study; and (ii) statistical analysis using six performance indices (CC, E^2, MAE, MSE, MRSE, MAPE;) computed over the aggregate dataset of n = 78 observed-computed pairs drawn from all six case studies. This dual-method validation framework ensures that both the spatial trend (graphical) and the overall quantitative agreement (statistical) of the model are assessed consistently and reproducibly.

6. Performance of the IEC 62364 (2019) equation

The IEC 62364:2019 standard provides an empirical framework for hydro abrasive erosion in various hydraulic machines or turbines[52]. It considers sediment characteristics, operating conditions, and material properties to predict erosion rates at critical turbine components. The main advantage of this standard is that it offers a unified methodology applicable to Kaplan, Francis, and Pelton turbines. However, its performance in practical applications depends mainly on how well input parameters are calibrated to site specific conditions.

In this study, we collected the six expressions proposed by previous investigators, as shown in Equation (1)-(6). Data were collected for verification only from those studies that follow the IEC 62364 equation. The accuracy of the IEC 62364 equation using both graphical and statistical methods was checked and verified. In Figure 5 (a-h), the X-axis represents the computed erosion. In contrast, the Y-axis represents the observed erosion at various parts of the turbine, including the blade tip, blade outlet, and blade chamber, and it also shows the percentage error (±25%) between the observed and computed erosion.

6.1 Kaplan turbine

Arora et al[17] applied the IEC 62364[24] erosion model to a low head Kaplan turbine and reported the predicted wear rate that closely matches the observed pattern as shown in Figure 5(a). The model predicts erosion at the blade tip of approximately 0.88 to 1.37 mm/year, blade outlet erosion of 2.4 to 3.74 mm/year, and guide vane wear of up to 0.01 to 1.53mm/year[17]. These values imply that the trailing edges of the blades and the upper chamber experience the greatest loss, in agreement with field measurements. For example, predicted tip wear (~1 mm/year) and outlet wear (~3 mm/year) fall in the same range as the roughly millimetre scale erosion depths seen in practice. Thus, the IEC model's output for the Kaplan case is qualitatively aligned with observed trends: blade tip and outlet regions show the highest erosion, the runner chamber is moderately affected, and guide vanes experience comparatively low wear. In short, the calculated erosion rates are of the same order as the measured rates, confirming that the model can capture the key erosion hotspots in Kaplan units.

Rai & Kumar[16] also examined Kaplan turbine erosion, as presented in Figure 5(c). Their results revealed a broader scatter of data points, particularly at the turbine outlet, suggesting overprediction attributable to the simplified empirical treatment of sediment impact and flow conditions at the time. Data points in Figure 5(c) extend beyond the ±25% error band at the blade outlet under extended operational durations, which is consistent with the IEC model's limitation in representing cumulative wear dynamics under nonlinear temporal erosion trajectories.

6.2 Francis Turbines

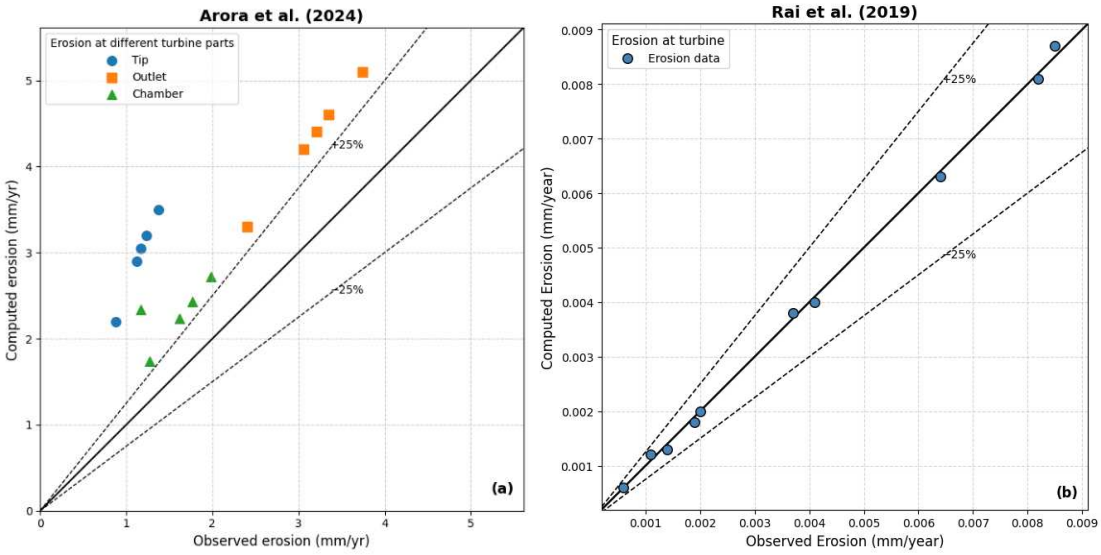
Acharya et al[25] analysed the Francis turbine from a Himalayan run of river plant and compared IEC-derived predictions with overhaul measurements. They found excellent agreement for the significant components as shown in Figure 5(d). For a 229 h operational period, guide vanes

(facing plates) suffered an observed abrasion depth of 8.1 mm. In comparison, the IEC 62364[24] predicted 7.53 mm. Similarly, the labyrinth seal (runner outlet clearance) exhibited a measured wear of 1.5 mm, compared to a calculated wear of 1.89 mm [25]. These numbers indicate only minor deviations between considering the model and the field, especially given site variability. (Runner inlet and outlet regions were predicted to erode modestly as well, though detailed values were not reported.) Overall, the IEC 62364[24] predictions align with the measured hierarchy: the guide vanes experience the heaviest wear (on the order of several millimetres), labyrinth seals wear moderately, and runner blades exhibit lesser erosion. Acharya's study thus concludes that the model's estimates "show good correlation" with field data. Figure 5(g) further illustrates the validation results reported by Acharya et al.[25], where the predicted erosion depths closely match the corresponding field measurements for all major Francis turbine components. The close clustering of the data around the 1:1 agreement line, with all points remaining within the ±25% acceptance limits, confirms the satisfactory predictive capability of the IEC 62364:2019 model under prototype operating conditions. Sangal et al[26] provided further corroboration through multi-zone validation across guide vanes, runner inlets/outlets, and labyrinth seals, as shown in Figure 5(f). Further Figure 5(h) demonstreates the predictive performance of the IEC 62364:2019 model using 20 observed computed erosion pair reported by sangal et al[53].the predicted erosion depth exhibit strong agreement with measured value over broad erosion range (2-78), with validation points confined within the ±25% acceptance envelope of the 1:1 agreement line. The observed agreement confirms the robustness and general applicability of the model for predicting hydro-abrasive erosion in Francis turbine components under prototype operating conditions. The results exhibited very tight clustering around the 1:1 line, with deviations rarely exceeding ±10–15%, confirming the robustness of their physics-informed CFD erosion coupling approach. Sharma et al[50] provided corroborative evidence from a dataset of sixteen data points drawn from modern turbine geometries, as

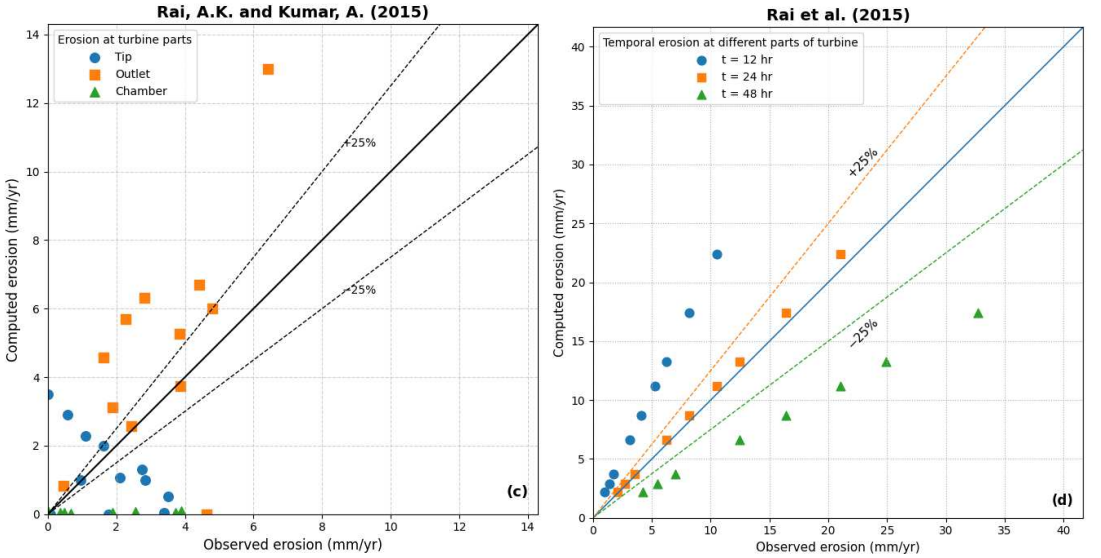
423 presented in Figure 5(e). While sixteen data points are limited for statistically robust standalone
424 validation of any model in isolation, their close alignment with the 1:1 line and inclusion within
425 the aggregate multi-study framework of n = 78 pairs provides supporting evidence for the IEC
426 model's calibration accuracy, and they are treated accordingly in the combined statistical
427 analysis.

428 **6.3 Pelton Turbines**

429 Field studies of high head Pelton plants have documented extreme injector erosion, and the
430 IEC model similarly identifies the nozzle or spear system as the critical wear zone. For instance,
431 investigations have found erosion rates on the order of 3 to 4 mm/year on the bucket splitters
432 and the spear of a Pelton jet. One report estimates an average wear rate of about 3.4 mm/year
433 for a bucket and needle combination in a Himalayan Pelton unit[54]. In contrast, the buckets
434 themselves may see only ~0.1 mm/year on average[55]**.** This pattern, characterised by severe
435 wear at the spear/nozzle and relatively mild wear on the buckets, is consistent with the IEC
436 model expectations for Pelton turbines. The model predicts the most significant sediment
437 impact at the nozzle exit and spear tip, in line with Sharma's observations that these parts are
438 eroded most aggressively, as shown in Figure 5 (e). While we lack published IEC model
439 erosion rates in the Pelton case, the qualitative agreement is explicit. Both measurements and
440 theory assign the highest wear to the injector (needle and nozzle) and much lower erosion to
441 the runner buckets and cutouts. Any numerical discrepancies are primarily due to the extreme
442 variability in head and sediment load. In practice, the IEC model appears to capture the general
443 erosion trend in Pelton turbines (peak wear at the nozzle/spear), though exact values would
444 require site specific calibration.

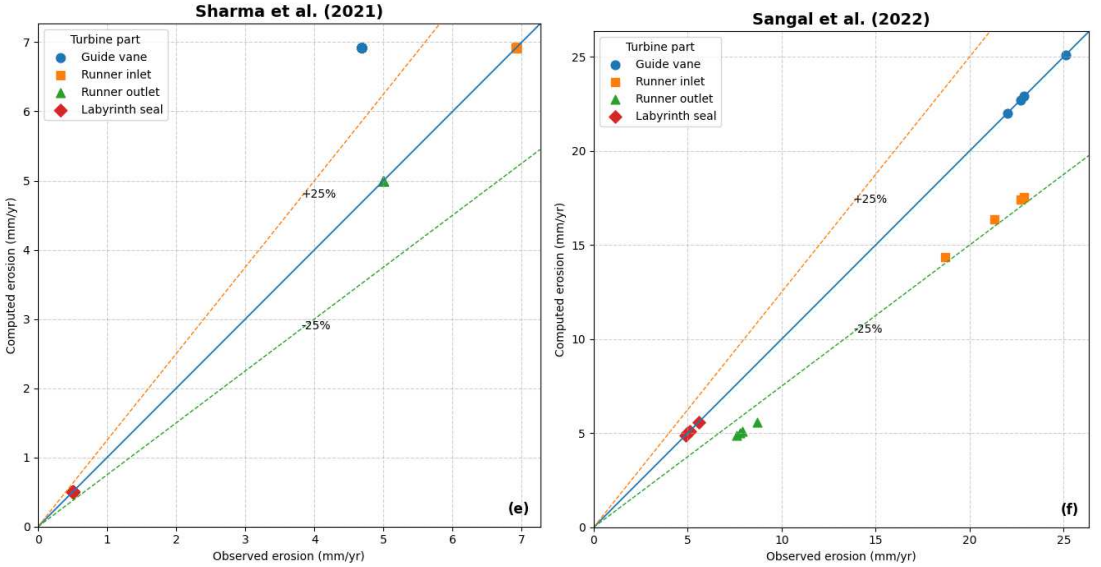


445

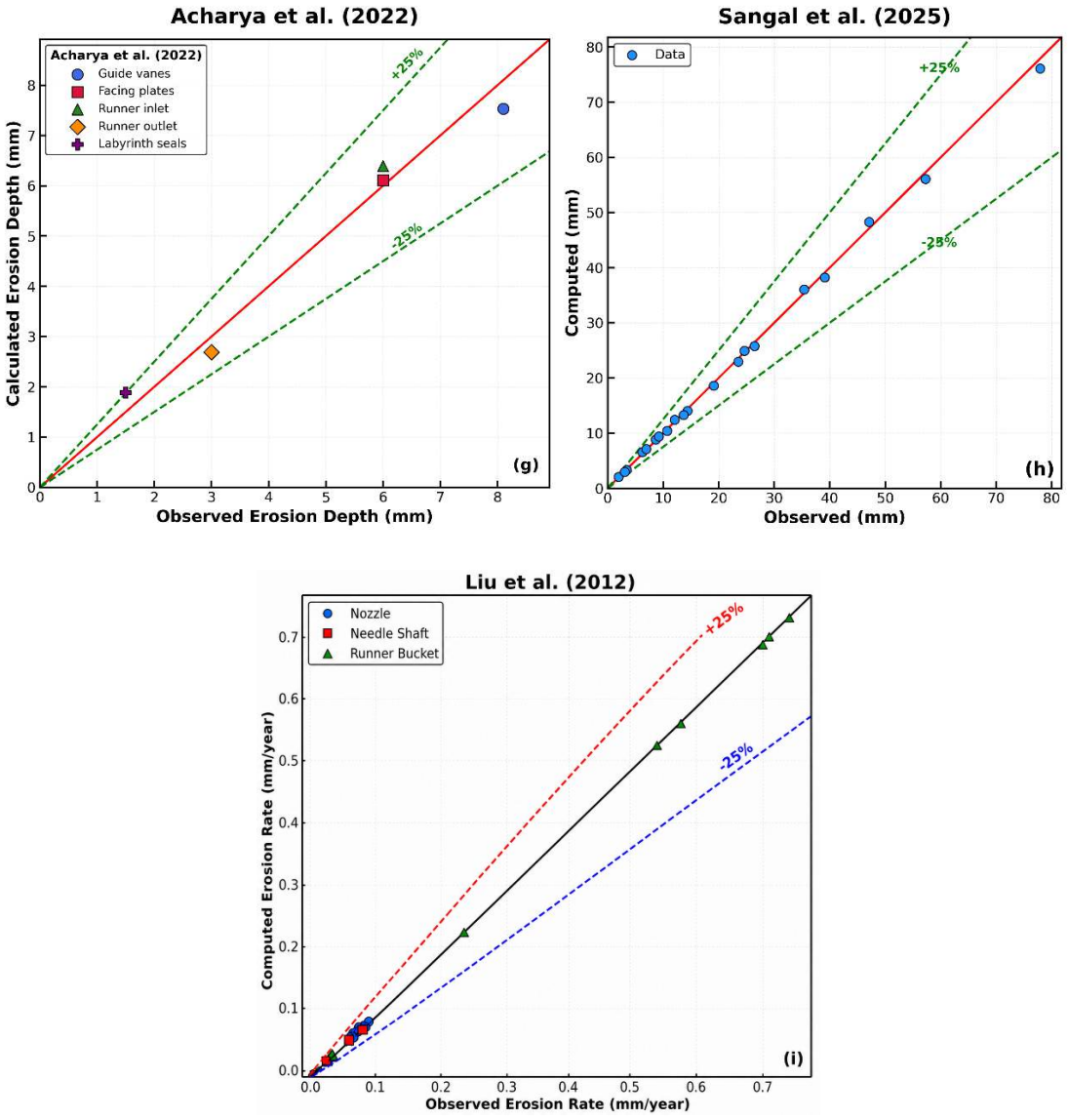


446

447



448



449

450

451

452 **Figure 5** (a to f) Observed versus computed erosion using a) Arora et al[17] b) Rai et al[56] c) Rai,
453 A.K., & Kumar[57] d) Rai et al [51] e) Sharma et al[50] f) Sangal et al[26] g) Acharya et al[54] h)Sangal
454 et al[53]i)Lie et el[58].

455 The comparative evaluation of the computed versus observed erosion plots from various
456 studies (Arora et al[17] , Rai et al[56], Rai, A.K., & Kumar[57], Rai et al[51] , Sharma et al[50], Sangal[26]
457 Acharya et al[54] Sangal et al[53]., Lie et el[58]) collectively demonstrates the progressive refinement
458 of turbine erosion prediction models over the past decade. In all cases, the 1:1 line represents
459 perfect agreement between computed and measured erosion rates, while the ±25% dashed
460 envelopes denote acceptable prediction uncertainty. The earliest validation by Rai & Kumar[16]

reveals a broader scatter of data points, particularly at the turbine outlet, suggesting overprediction due to the simplified empirical treatment of sediment impact and flow conditions. In contrast, Rai et al[57] extended this work by including temporal variation (12-48 h of exposure), which revealed a nonlinear erosion progression, with computed values increasing faster than observed under prolonged operation, highlighting model limitations in representing cumulative wear dynamics.

The later work by Rai et al[56] demonstrated substantial improvement, with nearly all data points lying within the $\pm 25\%$ confidence band at very low erosion magnitudes (as shown in Figure 5b; 10^{-3} mm/year range). This indicated that their refined model accurately captured micro scale erosion phenomena and was better suited for fine grained or low head turbine conditions. Subsequently, Sharma et al[50] provided corroborative evidence from a limited but high-quality dataset from modern turbine geometries. While comprising only Sixteen data points (Figure 5e), insufficient for statistically robust standalone validation, their close alignment with the 1:1 line offers preliminary confirmation of the IEC model's calibration accuracy and is treated as supporting evidence within the aggregate multi-study framework of this study. Sangal et al[26] further enhanced this approach through multi zone validation across guide vanes, runner inlets, outlets, and labyrinth seals. The results exhibited very tight clustering around the 1:1 line, with deviations rarely exceeding ±10–15%, confirming the robustness of their physics informed CFD erosion coupling approach.

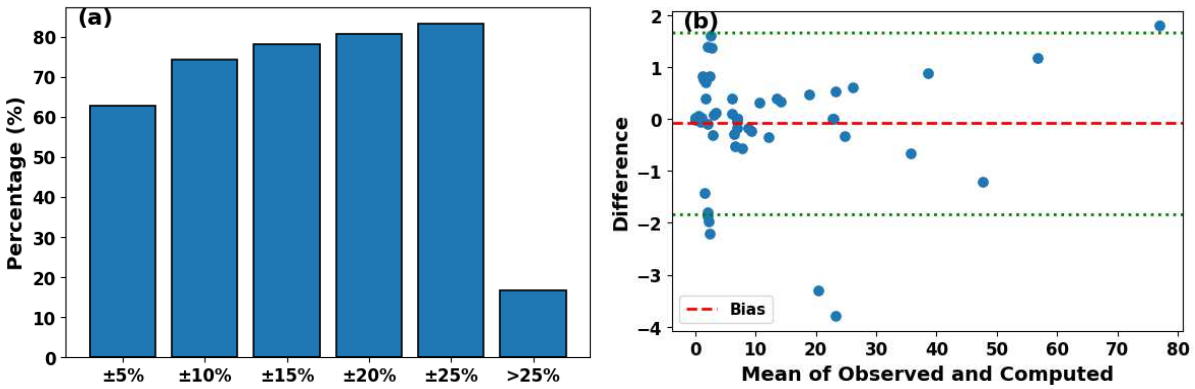
Similarly, the validation using the experimental dataset of Lie et el[58] (Figure 5i) shows close agreement between the computed and observed erosion rates for the nozzle, needle shaft, and runner bucket. Most data points cluster tightly around the 1:1 line and fall within the ±25% error limits, pointing to reliable predictions across different turbine components. The limited scatter, along with the absence of any systematic over or under-prediction, speaks to the

485 robustness of the computational model — a conclusion further backed by strong statistical
486 performance.

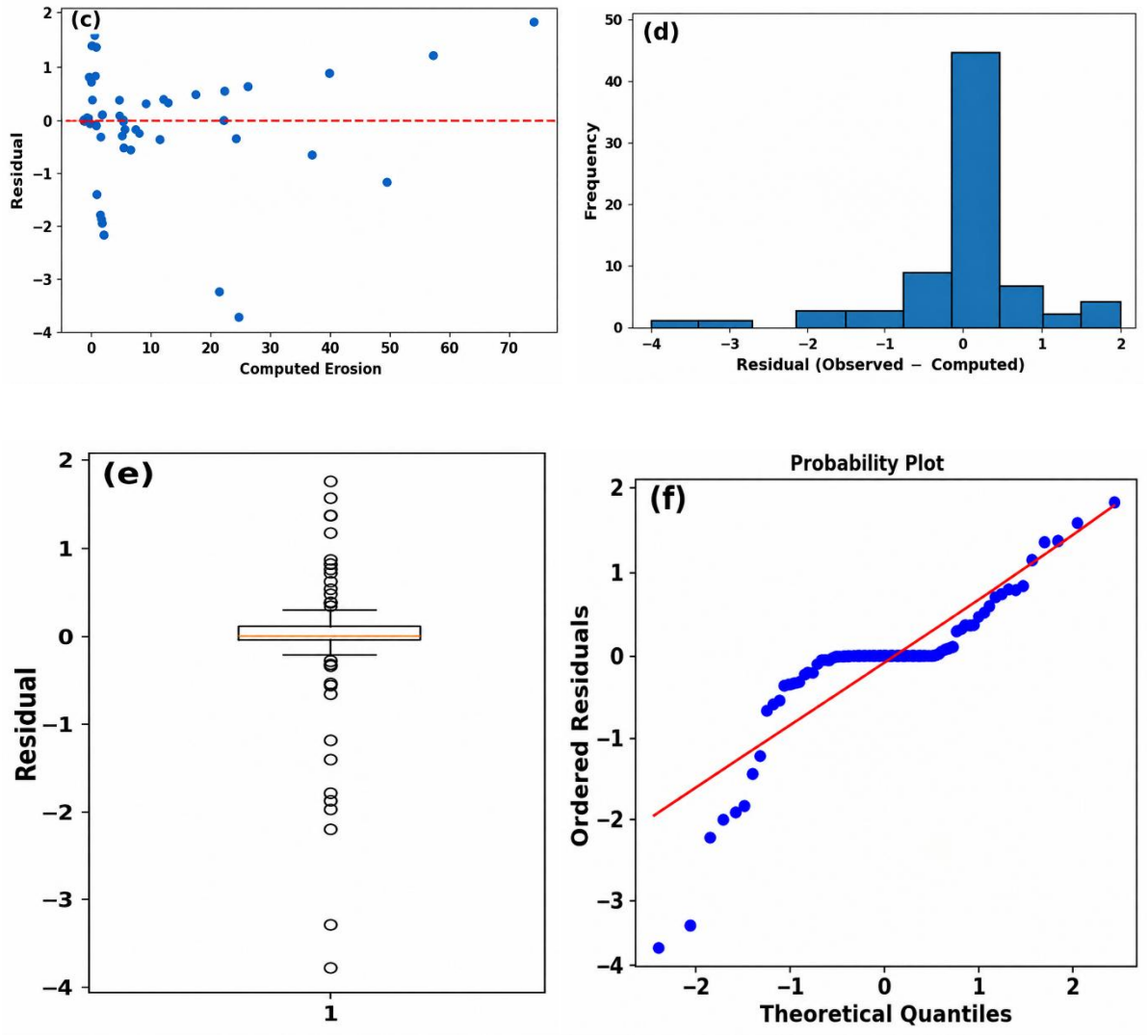
487 The most recent study by Arora et al[17] represents the culmination of these advancements. Their
488 results for the tip, outlet, and chamber regions showed high consistency within the ±25% limits,
489 with only minor overprediction observed. The reduced scatter, together with the near-
490 symmetric deviation around the 1:1 line, suggests improved spatial resolution of flow-particle
491 interactions and a more realistic representation of sediment loading. Overall, this comparative
492 analysis establishes that erosion prediction models have evolved from empirical and semi
493 empirical approximations toward fully coupled CFD based frameworks that capture the spatial
494 and temporal variability of wear more accurately. The consistency of results within ±25%
495 across diverse studies confirms the maturity and reliability of contemporary computational
496 approaches for turbine material loss assessment in sediment laden hydropower systems.

497 **6.4 Statistical Validation and Residual Error Analysis**

498 To further evaluate the predictive reliability of the IEC 62364:2019 model , a comprehensive
499 statical validation was perform using error band analysis, Bland –Altman analysis , residual
500 dignostics, histogram, boxt plot and normal probability (Q–Q) plot, as illustrated in Figure 6(a–
501 f). These complementary statistical techniques provide a comprehensive assessment of the
502 model accuracy, prediction uncertainty, residual characteristics, and agreement between the
503 experimentally observed and IEC 62364:2019 model-computed erosion values.



504



505

506

507 **Figure 6. Comprehensive statistical validation of the IEC 62364:2019 model for**
508 **predicting hydro-abrasive erosion in hydraulic turbines: (a)** cumulative error band
509 analysis, **(b)** Bland–Altman agreement plot, **(c)** residuals versus computed erosion, **(d)** residual
510 histogram, **(e)** residual boxplot, and **(f)** normal Q–Q plot of residuals.

511 The quantitative outcomes of the statistical validation are summarised in Table 8, which
512 complements the graphical analyses presented in Figure 6(a–f). The table provides an
513 integrated summary of the predictive performance of the IEC 62364:2019 model based on
514 conventional statistical indices, error band analysis, agreement assessment, and residual
515 diagnostics.

516 **Table1** Summary of the statistical validation results used to evaluate the predictive
517 performance of the **IEC 62364:2019** model for hydro-abrasive erosion in hydraulic turbines.

Statistical Analysis	Performance Metric	Result	Interpretation
Error Band Analysis	Predictions within ±5%	63%	Model predictions are highly accurate at this tight tolerance
	Predictions within ±10%	74%	Agreement between predicted and observed values remains strong
	Predictions within ±15%	78%	Predictions align well with observed erosion trends
	Predictions within ±20%	81%	Accuracy at this level meets typical engineering standards
	Predictions within ±25%	83%	Model performs well within acceptable engineering tolerances
	Predictions outside ±25%	17%	Only a small fraction of predictions deviate substantially
Bland–Altman Analysis	Mean bias	≈ 0	The model shows no consistent tendency to over- or under-predict
	95% limits of agreement	Majority of observations within limits	Predicted and observed erosion values largely align
Residual Analysis	Residual distribution	Random around zero	Errors appear random rather than following a consistent pattern
	Residual trend	No discernible pattern	Prediction errors don't scale with erosion magnitude
Residual Histogram	Residual concentration	Majority near zero	Most predictions carry only minor error, reflecting low uncertainty
Residual Boxplot	Residual spread	Narrow interquartile range with few outliers	The model behaves consistently, with few extreme deviations
Normal Q–Q Plot	Residual normality	Approximate normal distribution	Residuals reasonably meet the assumptions needed for statistical validity

518

519

The error band analysis (Figure 6(a)) shows that approximately 63% of the computed erosion values fall within ±5% of the observed measurements, while the prediction coverage progressively increases to 74%, 78%, 81%, and 83% within the ±10%, ±15%, ±20%, and ±25% error bands, respectively. Only 17% of the predictions exceed the ±25% error threshold, indicating that the IEC 62364:2019 model provides reliable erosion estimates with acceptable engineering accuracy over a broad range of operating conditions.

The Bland–Altman plot and residual analysis (Figure 6(b–c)) further demonstrate the predictive reliability of the model. The mean bias is close to zero, and most observations lie within the 95% limits of agreement, indicating excellent agreement between the observed and computed erosion values. Furthermore, the residuals are randomly distributed about the zero reference line without any discernible trend, suggesting that the prediction errors are unbiased and independent of the erosion magnitude, with no evidence of systematic overprediction or underprediction.

The residual histogram, boxplot, and Q–Q plot (Figure 6(d–f)) indicate that the residuals are predominantly centred around zero with a relatively narrow spread, although a few outliers are observed. The Q–Q plot further shows that the residuals closely follow the theoretical normal distribution, with only minor deviations at the distribution tails that are attributable to a limited number of extreme observations. Such deviations are expected in sediment-induced erosion studies because of the inherent variability associated with sediment transport, particle impacts, and local hydraulic conditions.

Overall, the statistical analyses presented in Figure 6(a–f) demonstrate that the IEC 62364:2019 model provides accurate, unbiased, and statistically consistent predictions of hydro-abrasive erosion. The high proportion of predictions within acceptable error bands, negligible mean bias, random residual distribution, and approximate normality of residuals collectively confirm the

robustness and practical applicability of the model for predicting erosion in Kaplan, Francis, and Pelton turbines under diverse operating conditions.

7. Statistical validation of (IEC 62364 2019) the equations.

The statistical validation presented in this section is based on the aggregate dataset comprising all observed versus IEC 62364:2019-computed erosion pairs collected from six published studies: (i) Arora et al[17]Kaplan turbine, Mohammadpur HPP, India - blade tip, outlet, and chamber components (n = 6 data pairs); (ii) Rai et al[56]-Kaplan turbine, low-head conditions-micro-scale erosion measurements (n = 5 data pairs); (iii)) Rai, A.K., & Kumar[57]- Kaplan turbine, India -blade inlet, outlet, and chamber components (n =12 data pairs); (iv) Rai et al [51]-Pelton turbine-temporal erosion measurements at 12, 24, and 48-hour exposure durations (n = 9 data pairs); (v) Sharma et al[50]-Francis turbine-guide vane, runner, faceplate, labyrinth seal (n = 16 data pairs); and (vi) Sangal et al[26]-Francis turbine, Bhilangana-III HEP -guide vane, runner inlet/outlet, chamber, labyrinth seal (n = 5 data pairs) (vii) Acharya et al[54] having the data set of 5 at different location of francis turbin and (viii) Sangal et al[53] – francis turbine with number of datra 20 . The total dataset, therefore, comprises n = 78 observed-computed erosion pairs spanning three turbine types (Kaplan, Francis, Pelton) and a range of erosion magnitudes (10^{-3} to 10^{1} mm/year). It should be noted that the size of the dataset is relatively limited because only a small number of researchers have reported detailed field measurements of turbine erosion along with the information required for applying the IEC 62364:2019 model. Despite this limitation, the compiled dataset represents the most comprehensive set of publicly available erosion observations currently accessible for evaluating the predictive capability of the model across different turbine types and operating conditions. Statistical analysis used to verify the accuracy of the IEC 62364[24] model. The degree of agreement between the calculated and observed hydro abrasive erosion was determined using six statistical indices shown in Equations (7)-(12), namely the Correlation Coefficient (CC) and the Coefficient of

Determination. E^2, Mean Absolute Error (MAE), Mean Squared Error (MSE), Root Mean Squared Error (RMSE), and Mean Absolute Percentage Error (MAPE), where Z is the observed value and Z' is the corresponding calculated value[59].

Correlation Coefficient (CC)

$$CC = \frac{n\sum ZZ' - \sum Z \sum Z'}{\sqrt{n\sum Z^2 - (\sum Z)^2}\ \sqrt{n\sum Z'^2 - (\sum Z')^2}} \quad (7)$$

Efficiency of correlation (E^2)

$$E^2 = \frac{\sum_{i=0}^{n}\left(Z_i - \overline{Z_i}\right)^2 - \sum_{i=1}^{n}(Z_i - Z'_i)^2}{\sum_{i=1}^{n}\left(Z_i - \overline{Z_i}\right)^2} \quad (8)$$

Mean Absolute Error (MAE)

$$MAE = \frac{1}{n}\sum_{i=1}^{n}|Z_i - Z'_i| \quad (9)$$

Mean Square Error (MSE)

$$MSE = \frac{1}{n}\sum_{i=1}^{n}(Z_i - Z'_i)^2 \quad (10)$$

Mean Root Square Error (MRSE)

$$MRSE = \sqrt{\frac{\sum_{i=1}^{n}(Z_i - Z'_i)^2}{n}} \quad (11)$$

Mean Absolute Percentage Error (MAPE)

$$MAPE = \frac{100}{n}\sum_{i=1}^{n}\frac{|Z_i - Z'_i|}{|Z_i|} \quad (12)$$

The statistical analysis of the suggested erosion model demonstrates high predictive power [60]. Perfect linear agreement between observed and anticipated erosion values is indicated by the correlation coefficient, $CC = 0.997$, indicating that the model successfully replicates the experimental trend. Similarly, the model's robustness in capturing the erosion mechanism is

demonstrated by the Efficiency of correlation E^2, which equals 0.99.5, indicating that the model accounts for over 99.5% of the variance in the measured data.

The error based measures further confirm the model's dependability. Given the inherent uncertainties in erosion measurements, the $MAE\ of\ 0.47$indicates that projections often differ from experimental results by less than one unit. The relatively small residuals are reflected in the $MSE\ of\ 0.68$ and the $MRSE\ of\ 0.89$. This indicates that significant deviations are uncommon and the model remains stable under various operating conditions.

However, compared to the other indices, the $MAPE\ of\ 24.21$ is relatively high. This is explained by MAPE's sensitivity at low experimental erosion levels, when even modest absolute variations result in disproportionately high percentage errors. Studies on hydro abrasive erosion often exhibit this tendency when the initial wear depths are relatively small and localised. The combination of high CC and E^2 values, along with low $MAE, MSE, and\ MRSE$, confirms the model's ability to accurately depict the erosion process. Although the relatively bigger $MAPE$ explain the intricate and nonlinear character of sediment–turbine interactions, it does not compromise the model's correctness. As a result, the statistical performance validates the model's suitability for predicting erosion and its possible application in sediment management and turbine design. Localised

Table 2 Statistical Evaluation of the Erosion Model

Statistical Index	Value	Interpretation in Erosion Study
CC	0.997	Indicate excellent agreement between predicted and observed erosion
E²	0.995	Explain 99.58% of the observed erosion variability, indicating excellent model ferformance

MAE	0.47	The average prediction error is less than one unit, which is acceptable for erosion datasets.
MSE	0.68	Indicate low overall prediction error and stable model performance
MRSE	0.89	Reflect low prediction error between measured and predicted erosion depth
MAPE	24.21	It exhibits a higher relative error for small erosion values, a standard limitation inherent in percentage-based indices.

8. Discussion

It is clear from the comparative analysis of erosion data from Kaplan, Francis, and Pelton turbines that the IEC 62364[24]model provides a useful framework for estimating hydro-abrasive wear in sediment-rich environments. Comparisons between observed and calculated erosion indicate that the model generally reproduces the spatial distribution and relative magnitude of material loss across different turbine components. For Kaplan turbines, both field observations and model predictions identify blade tips and outlet regions as the most erosion-prone locations, with erosion rates ranging from approximately 0.9 to 3.7 mm/year. Similarly, the guide vane and chamber regions exhibit comparatively lower erosion rates (<1.5 mm/year), consistent with the model predictions[17]. For Francis turbines, the predicted erosion depths correspond reasonably well with measured values, including severe wear at guide vanes (~8.1 mm/year) and moderate wear at labyrinth seals (~1.5–1.9 mm/year)[25,52,59]. The model also successfully captures the relative erosion susceptibility of Pelton turbine components, correctly identifying the spear, nozzle, and bucket splitter as the most vulnerable regions, while predicting minimal erosion on runner surfaces approx. 3- 4 mm/year while Although the runners themselves only erode about 0.1 mm/year, their long term deterioration aligns with

model predictions. This consistency implies that the model captures the governing effects of the impact angle and jet velocity on the erosion rate..

The statistical evaluation further supports the applicability of the model. The IEC 62364:2019 formulation explains approximately 99.58% of the variance in the compiled erosion dataset ($E^2 = 0.9958$), with a high correlation coefficient ($CC = 0.997$) and relatively low error metrics ($MAE = 0.47, MSE = 0.687, and\ MRSE = 0.89$). Although the MAPE is 24.21%, this value may partly reflect the sensitivity of percentage-based error metrics at low erosion magnitudes, where small absolute deviations produce comparatively large percentage errors. The statistical validation presented in Figure 6(a–f) provides additional evidence supporting the reliability of the IEC 62364:2019 model beyond the conventional performance metrics. The error band analysis indicates that approximately 83% of the predictions fall within ±25% of the observed erosion values, demonstrating satisfactory engineering accuracy across different turbine types. Furthermore, the Bland–Altman agreement analysis reveals a negligible mean bias and that most observations lie within the 95% limits of agreement, confirming good consistency between measured and predicted erosion. The residual diagnostics, including the residual distribution, histogram, boxplot, and normal Q–Q plot, show that the prediction errors are randomly distributed around zero with approximate normality and only a limited number of outliers. Collectively, these results indicate that the IEC 62364:2019 model provides statistically reliable and unbiased erosion predictions, thereby reinforcing its applicability for hydro-abrasive erosion assessment in hydraulic turbines.

Despite its overall satisfactory performance, an important limitation of the IEC 62364[23] framework is its assumption of linear temporal erosion progression. The particle load term (P_L) is calculated as a linear accumulation of concentration-weighted sediment exposure ($\sum c_i \cdot K_{size,i} \cdot K_{shape,i} \cdot K_{hardness,i} \cdot t_i$), implicitly assuming that erosion depth increases proportionally with

operating time[24]. However, experimental observations and field measurements, particularly those reported by Rai and Kumar[16], suggest that erosion often follows a nonlinear temporal trajectory. During the early stages of operation, surface roughening can enhance particle impacts and accelerate material removal. As erosion progresses, changes in component geometry alter local flow patterns, impact angles, and particle trajectories, resulting in a gradual reduction in erosion rates[23]. Consequently, the IEC model may overpredict erosion during extended operating periods, particularly in outlet regions, blade trailing edges, and other locations where significant geometric evolution occurs. This behaviour is reflected by several data points lying outside the ±25% agreement band in Figure 5(c).

Therefore, the IEC framework is most reliable for short- to medium-term assessments and for turbine components where erosion progresses approximately linearly and the flow field remains relatively stable, such as guide vanes and labyrinth seals. Conversely, caution should be exercised when applying the model to long-term erosion assessments, highly sediment-laden operating conditions, or components undergoing substantial geometric modification, as prediction uncertainty may increase under such circumstances[61,15]. Incorporating geometry-evolution corrections or coupling the IEC framework with CFD-based flow simulations represents a promising direction for improving long-term predictive capability.

Overall, the results indicate that the IEC 62364[24]equation serves as a useful first-order predictor of hydro-abrasive erosion across different turbine types. When calibrated using site-specific sediment characteristics, including suspended sediment concentration (SSC), particle size distribution (PSD), and sediment hardness, the model provides reasonable estimates of component-level wear and can support erosion assessment and maintenance planning in hydropower systems.

9. Conclusion

Sediment induced hydro abrasive erosion remains one of the most significant operational challenges for hydropower plants operating in rivers with high sediment loads, particularly in mountainous regions where rivers carry high concentrations of hard mineral particles, such as quartz and feldspar[62,63]. The present study has synthesised published field observations, experimental investigations, and modelling studies to examine erosion behaviour in the three dominant conventional hydraulic turbine types, Francis, Kaplan, and Pelton, and to evaluate the applicability of the IEC 62364[24] erosion estimation framework. The comparative analysis suggests that erosion behaviour is governed by by a combination of turbine geometry, sediment characteristics, and local hydraulic conditions. Francis turbines are especially susceptible to erosion at guide vanes, runner inlet and outlet regions, facing plates, and labyrinth seals, where complex three-dimensional flow structures and high turbulence intensify particle–surface interactions[9]. Kaplan turbines operating under low head and high discharge conditions commonly exhibit erosion at blade tips, trailing edges, and runner chambers due to elevated circumferential velocities and leakage flows[17],[57]. In contrast, Pelton turbines experience pronounced localised erosion at nozzles, spear needles, and bucket splitters as a result of direct impingement by high velocity sediment laden jets[8, 12].

A key finding of this serearch is the persistent gap between erosion observed in operating hydropower plants and that predicted using available modelling approaches. Although, several empirical and semi empirical erosion models have been proposed over the past decades[10,11] and their predictive capability is often limited by site specific sediment properties, turbine design, and operating conditions[64]. The IEC 62364[24] standard represents a significant step toward a unified and standardised framework for hydro abrasive erosion estimation, as it systematically incorporates sediment characteristics, turbine material properties, and hydraulic parameters[24]. However, the existing literature shows that applications of the IEC model are predominantly

limited to individual turbine types or isolated case studies, with relatively few systematic comparisons against observed erosion data. By compiling erosion data from multiple published field and experimental studies and comparing observed wear with IEC based predictions using consistent graphical and statistical approaches, this review highlights both the strengths and limitations of the IEC 62364[24] framework. While the model is generally capable of capturing overall erosion trends across different turbine types, with predictions falling within ±25% of observed values for the majority of components, including blade tips, guide vanes, runner inlets and outlets, and labyrinth seals, with approximately 83% of the compiled observations falling within the ±25% error band. The complementary statistical validation, including Bland–Altman agreement analysis and residual diagnostics, further confirmed that the IEC 62364:2019 model provides unbiased and statistically consistent erosion predictions with negligible systematic bias. Considering the complexity of hydro-abrasive erosion processes, the variability in sediment characteristics, and the practical challenges associated with experimental investigations and long-term field measurements, achieving prediction agreement within the ±25% error band represents a satisfactory level of engineering accuracy for this class of hydraulic systems. Experimental studies on hydro-abrasive erosion require prolonged operating durations, controlled sediment properties, and precise measurement of relatively small material losses under highly turbulent hydraulic conditions, making both experimentation and data acquisition inherently challenging. Therefore, the agreement obtained for approximately 83% of the compiled observations within the ±25% error band demonstrates the practical reliability and engineering applicability of the IEC 62364:2019 model. Nevertheless, notable exceptions are identified for outlet components under extended operational durations and under hydraulic conditions that promote nonlinear temporal wear progression. notable exceptions are identified for outlet components under extended operational durations and under hydraulic conditions that promote nonlinear temporal wear

progression. These discrepancies arise principally from the model's linear time-integration assumption, which cannot reproduce the acceleration-then-deceleration erosion trajectory consistently observed in field measurements. These findings underscore the importance of carefully interpreting model results, the need for ongoing validation using reliable, long-term field measurements, and the development of geometry-evolving correction factors within the IEC framework.

Overall, this review emphasises the importance of integrating field-observed erosion data with standardised predictive models to support informed turbine design, material selection, and maintenance planning. Future research should focus on expanding high quality field erosion datasets, improving sediment characterisation, and refining erosion prediction approaches to better represent local hydraulic and sediment dynamics. Such efforts are crucial for enhancing the reliability of erosion prediction and ensuring the long term performance and sustainability of hydropower plants operating in sediment-rich river environments.

Data Availability Statement

The datasets used and/or analyzed during the current study are available from the corresponding author on reasonable request

Reference

1. Wuebbles, D. J. & Jain, A. K. Concerns about climate change and the role of fossil fuel use. 99–119 (2001).
2. Lee, H. Climate Change 2023 Synthesis Report. 35–115 (2023) doi:10.59327/IPCC/AR6-9789291691647.
3. Akpasi, S. O., Michael, I., Anekwe, S., Tetteh, E. K. & Mustapha, S. I. Hydrogen as a clean energy carrier : advancements , challenges , and its role in a sustainable energy future. **9**, 52–88 (2025).
4. Frey, G. W. & Linke, D. M. Hydropower as a renewable and sustainable energy resource meeting global energy challenges in a reasonable way. **30**, 1261–1265 (2002).
5. Sangal, S., Singhal, M. K. & Saini, R. P. Hydro-abrasive erosion in hydro turbines: a

review. *International Journal of Green Energy* vol. 15 232–253 at https://doi.org/10.1080/15435075.2018.1431546 (2018).

6. Bajracharya, S. R., Mool, P. K. & Shrestha, B. R. Global Climate Change and Melting of Himalayan Glaciers Abstract : (2008).

7. Vishwakarma, R. & Pant, C. S. Field-based characterization and computational assessment of sediment erosion in Pelton turbine injectors at a Himalayan hydropower site. https://doi.org/10.1063/5.0284519 (2025) doi:10.1063/5.0284519.

8. *Thapa*. (2004).

9. Singh, B., Gunnar, O. & Thapa, B. Sediment erosion in hydro turbines and its effect on the fl ow around guide vanes of Francis turbine. *Renew. Sustain. Energy Rev.* **49**, 1100–1113 (2015).

10. Finnie, I. Erosion of surfaces. *Wear* **3**, 87–103 (1960).

11. Boes, R. M. Real-time monitoring of suspended sediment concentration and particle size distribution in the headwater way of a high-head hydropower plant IAHR Member , Prof . Dr ., Laboratory of Hydraulics , Hydrology and Glaciology ABSTRACT A suspended sediment monit. (2009).

12. Padhy, M. K. & Saini, R. P. A review on silt erosion in hydro turbines. **12**, 1974–1987 (2008).

13. Mack, R., Drtina, P. & Lang, E. Numerical prediction of erosion on guide vanes and in labyrinth seals in hydraulic turbines. *Wear* **233**–**235**, 685–691 (1999).

14. Sharma, S. & Gandhi, B. K. Assessment of erosion wear in low specific speed Francis turbine due to particulate flow. *Adv. Powder Technol.* **34**, 104065 (2023).

15. Sangal, S., Singhal, M. K. & Saini, R. P. Hydro-abrasive erosion in hydro turbines : a review. **5075**, (2018).

16. Rai, A. K. & Kumar, A. Analyzing hydro abrasive erosion in Kaplan turbine : A case study from India *. *J. Hydrodyn.* **28**, 863–872 (2016).

17. Arora, N., Kumar, A. & Singal, S. K. Hydro-abrasive erosion in Kaplan turbines: a case study. *J. Hydroinformatics* https://doi.org/10.2166/hydro.2024.096 (2024) doi:10.2166/hydro.2024.096.

18. Han, L. *et al.* Effects of sediment characteristics on the erosion of Pelton turbine. *J. Hydraul. Res.* **62**, 236–252 (2024).

19. Wang, J. *et al.* Research on Soil Erosion Based on Remote Sensing Technology : A Review. 1–31 (2025).

20. Igwe, P. U., Onuigbo, A. A., Chinedu, O. C., Ezeaku, I. I. & Muoneke, M. M. Soil Erosion : A Review of Models and Applications. **6495**, 138–150 (2017).

21. Truscott, G. F. 29 a literature machinery* survey on abrasive wear in hydraulic. **20**, (1972).

22. Krallis, G. & Edinger, J. Sediment Transport Modeling Review — Current and. **134**, 1–14 (2008).

23. Padhy, M. K. & Saini, R. P. Effect of size and concentration of silt particles on erosion

of Pelton turbine buckets. *Energy* **34**, 1477–1483 (2009).

24. 62364, I. *INTERNATIONAL STANDARD*. (2019).

25. Acharya, N., Gautam, S., Chitrakar, S., Trivedi, C. & Dahlhaug, O. Application of hydro-abrasive erosion model from IEC 62364 : 2019 standard in Francis turbines Application of hydro-abrasive erosion model from IEC 62364 : 2019 standard in Francis turbines. https://doi.org/10.1088/1755-1315/1079/1/012008 (2022) doi:10.1088/1755-1315/1079/1/012008.

26. Sangal, S., Kumar Singhal, M., Prasad Saini, R. & Singh Tomar, G. Hydro-abrasive erosion modelling in Francis turbine at different silt conditions. *Sustain. Energy Technol. Assessments* **53**, (2022).

27. Shrestha, R. *et al.* Review on experimental investigation of sediment erosion in hydraulic turbines. *Front. Mech. Eng.* **10**, (2024).

28. Singh, J., Singh Chohan, J., Hameed Hlail, S. & Kumar Saxena, K. Future perspective on the flow disturbances in Francis turbine caused by sediment particles and implementation of protection technique. *Mater. Today Proc.* https://doi.org/10.1016/j.matpr.2023.09.118 (2023) doi:10.1016/j.matpr.2023.09.118.

29. Shrivastava, N. & Rai, A. K. Hydro-abrasive erosion in Pelton turbines: Comprehensive review and future outlook. *Renewable and Sustainable Energy Reviews* vol. 207 at https://doi.org/10.1016/j.rser.2024.114957 (2025).

30. Rai, A. K., Kumar, A., Staubli, T. & Yexiang, X. Interpretation and application of the hydro-abrasive erosion model from IEC 62364 (2013) for Pelton turbines. *Renew. Energy* **160**, 396–408 (2020).

31. Zehab, M., Din, U. & Harmain, G. A. Assessment of erosive wear of Pelton turbine injector : Nozzle and spear combination – A study of Chenani hydro-power plant. *Eng. Fail. Anal.* **116**, 104695 (2020).

32. Lu, X. *et al.* Investigation of Sediment Erosion of the Top Cover in the Francis Turbine Guide Vanes at the Genda Power Station. *J. Mar. Sci. Eng.* **13**, 1–23 (2025).

33. Nguyen, V. B., Nguyen, Q. B., Zhang, Y. W., Lim, C. Y. H. & Khoo, B. C. Effect of particle size on erosion characteristics. *Wear* **348**–**349**, 126–137 (2016).

34. Uzi, A. & Levy, A. On the relationship between erosion, energy dissipation and particle size. *Wear* **428**–**429**, 404–416 (2019).

35. An, W. *et al.* A Review: Factors Controlling Erosion Resistance in Metals Prioritizing the Influence of Material Mechanics and the Related Erosion Models. *Metals (Basel).* **15**, 1–30 (2025).

36. Narváez, M., Guamán, J., Hidalgo, V. H., Pérez-Sánchez, M. & Ramos, H. M. Lagrangian Simulation of Sediment Erosion in Francis Turbines Using a Computational Tool in Python Coupled with OpenFOAM. *Machines* **13**, 1–25 (2025).

37. Arora, N., Kumar, A. & Singal, S. K. Technological advancement in measurements of suspended sediment and hydraulic turbine erosion. *Measurement* **190**, 110700 (2022).

38. Bhattarai, A., Kunwar, P., Chitrakar, S. & Gautam, S. Investigation of sediment erosion in low head Francis turbines and its effect on the structural integrity. *IOP Conf.*

Ser. Earth Environ. Sci. **1037**, (2022).

39. Ghenaiet, A. Simulating Sediment Erosion in a Small Kaplan Turbine. *Int. J. Turbomachinery, Propuls. Power* **10**, (2025).

40. Wang, C., Tan, L., Chen, M., Fan, H. & Liu, D. A review on synergy of cavitation and sediment erosion in hydraulic machinery. *Front. Energy Res.* **10**, 1–23 (2022).

41. Padhy, M. K. & Saini, R. P. Study of silt erosion mechanism in Pelton turbine buckets. *Energy* **39**, 286–293 (2012).

42. Nobilo, M., Salehi, S. & Nilsson, H. Lifetime analysis of hydro turbines with focus on fatigue damage in a renewable energy system – A review. *Renew. Sustain. Energy Rev.* **228**, 116578 (2026).

43. Strategies, M., Singh, H. & Strategies, M. E- AT. (2026).

44. Liu, J., Yu, J. & Jiang, C. Evaluation on sediment erosion of Pelton turbine flow passage component Evaluation on sediment erosion of Pelton turbine flow passage component. https://doi.org/10.1088/1755-1315/240/2/022027 (2019) doi:10.1088/1755-1315/240/2/022027.

45. Vieira, R. E., Mansouri, A., Mclaury, B. S. & Shirazi, S. A. Experimental and computational study of erosion in elbows due to sand particles in air fl ow. **288**, 339–353 (2016).

46. Oka, Y. I., Okamura, K. & Yoshida, T. Practical estimation of erosion damage caused by solid particle impact Part 1 : Effects of impact parameters on a predictive equation. **259**, 95–101 (2005).

47. Zhang, Y., Reuterfors, E. P., Mclaury, B. S., Shirazi, S. A. & Rybicki, E. F. Comparison of computed and measured particle velocities and erosion in water and air flows. **263**, 330–338 (2007).

48. Sun, J. *et al.* Quantitative evaluation of yaw-misalignment and aerodynamic wake induced fatigue loads of offshore Wind turbines. *Renew. Energy* **199**, 71–86 (2022).

49. Gilchrist, A. Erosion by a stream of solid particles. (1968).

50. Sharma, S., Gandhi, B. K. & Pandey, L. Measurement and analysis of sediment erosion of a high head Francis turbine : A field study of Bhilangana-III hydropower. **122**, 1–20 (2021).

51. Rai, A. K., Kumar, A. & Staubli, T. DEVELOPING A TEST RIG TO MEASURE HYDRO-ABRASIVE EROSION IN PELTON DEVELOPING A TEST RIG TO MEASURE HYDRO-ABRASIVE EROSION IN PELTON TURBINE. (2015).

52. Sangal, S., Singhal, M. K. & Saini, G. P HYSICAL J OURNAL Sensitivity analysis of IEC 62364 erosion model in predicting hydro-abrasive erosion in Francis turbine : a case study of Maneri Bhali-II hydropower plant , India. *Eur. Phys. J. Spec. Top.* **123**, (2025).

53. Sangal, S., Singhal, M. K. & Saini, G. P HYSICAL J OURNAL Sensitivity analysis of IEC 62364 erosion model in predicting hydro-abrasive erosion in Francis turbine : a case study of Maneri Bhali-II hydropower plant , India. *Eur. Phys. J. Spec. Top.* **234**, 7389–7405 (2026).

54. Bajracharya, T. R., Acharya, B., Joshi, C. B., Saini, R. P. & Dahlhaug, O. G. Sand erosion of Pelton turbine nozzles and buckets : A case study of Chilime Hydropower Plant. **264**, 177–184 (2008).

55. Ge, X. *et al.* Sediment Erosion on Pelton Turbines : A Review. *Chinese J. Mech. Eng.* https://doi.org/10.1186/s10033-023-00880-y (2023) doi:10.1186/s10033-023-00880-y.

56. Rai, A. K. & Kumar, A. Determination of the particle load based on detailed suspended sediment measurements at a hydropower plant. *Int. J. Sediment Res.* **34**, 409–421 (2019).

57. Rai, A. K. & Kumar, A. Continuous measurement of suspended sediment concentration : Technological advancement and future outlook. *MEASUREMENT* **76**, 209–227 (2015).

58. Liu; J.; Lu; L.; & Zhu; Experiment study on sediment erosion of Pelton turbine flow passage component material Experiment study on sediment erosion of Pelton turbine flow passage component material. https://doi.org/10.1088/1755-1315/15/3/032055 (2012) doi:10.1088/1755-1315/15/3/032055.

59. Pandey, M., Sharma, P. K., Ahmad, Z. & Singh, U. K. Evaluation of existing equations for temporal scour depth around circular bridge piers. *Environ. Fluid Mech.* https://doi.org/10.1007/s10652-017-9529-9 (2017) doi:10.1007/s10652-017-9529-9.

60. Masoud, S., Reza, H. & Zare, M. Catena A comparative assessment of gully erosion spatial predictive modeling using statistical and machine learning models. *Catena* **207**, 105679 (2021).

61. Neopane, H. P. The effect of sediment characteristics for predicting erosion on Francis turbines blades. 79–83 (2012).

62. Raqib Qaderi, A., Chitrakar, S., Prasad Neopane, H. & Gunnar Dahlhaug, O. Comprehensive Review of Sediment Erosion Mechanisms and Their Impact on Francis Turbines. *IOP Conf. Ser. Earth Environ. Sci.* **1533**, (2025).

63. Felix, D., Albayrak, I. & Boes, R. M. Continuous measurement of suspended sediment concentration : Discussion of four techniques. *Measurement* **89**, 44–47 (2016).

64. Roughness, L. & Cheng, N. Estimate of Friction Factor for Flows Subject to.

Author Contributions

S.S.: conceptualisation, resources, data collection, data curation, formal analysis, statistical analysis, validation, original draft preparation, writing, review, and Editing. M.P.: provided the research idea,conceptualisation guidance, Review and editing , Validation continuous supervision throughout the study. N.A.: review and regular monitoring of the research work.

Funding:

The authors declare that no funds, grants, or other financial support were received during the preparation of this manuscript.